Asymmetric Sequential Cu-Catalyzed 1,6/1,4-Conjugate Additions of Hard Nucleophiles to Cyclic Dienones: Determination of Absolute Configurations and Origins of Enantioselectivity

Charlie Blons, Marie S. T. Morin, Thibault E. Schmid, Thomas Vives, Sophie Colombel-Rouen, Olivier Baslé, Thibault Reynaldo, Cody L. Covington, Stéphanie Halbert, Sean N. Cuskelly, et al.

Asymmetric Sequential Cu-Catalyzed 1,6/1,4 Conjugate Additions of Hard Nucleophiles to Cyclic Dienones. Determination of Absolute Configurations and Origins of Enantioselectivity

Charlie Blons,[a] Marie S. T. Morin,[a] Thibault E. Schmid,[a] Thomas Vives,[a] Sophie Colombel-Rouen,[a] Olivier Baslé,[a] Thibault Reynaldo,[b] Cody L. Covington,[c] Stéphanie Halbert,[d] Sean N. Cuskelly,[e] Paul V. Bernhardt,[e] Craig M. Williams,*[e] Jeanne Crassous,*[b] Prasad L. Polavarapu,*[c] Christophe Crévisy,*[a] Hélène Gérard*[d] and Marc Mauduit*[a]

Abstract: The first stereo-controlled Cu-catalyzed sequential 1,6/1,4-asymmetric conjugate addition (ACA) of C-metalated hard nucleophiles to cyclic dienones is reported. The use of DiPPAM, followed by a phosphoramidite, as the stereoinducing ligands facilitated both high ee's for the 1,6-ACA and high de's for the 1,4-ACA reaction components, thus affording enantio-enriched 1,3-dialkylated moieties. The absolute configurations were determined using vibrational circular dichroism (VCD) and optical rotatory dispersion (ORD) spectroscopy, in combination with DFT calculations and X-Ray analysis. Interestingly, DFT calculations of the mechanism for the enantioselective 1,6-addition via an unprecedented Cu-Zn bimetallic catalytic system confirmed this attribution. Lastly, exploring intramolecular cyclisation avenues on enantio-enriched 1,3-dialkylated products provided access to the challenging drimane skeleton.

Introduction

Copper-catalyzed Asymmetric Conjugate Addition (ACA) to electron-deficient conjugate polyenes holds great potential for the installation of otherwise difficult C-C bonds, provided that the regiochemical outcome of the process is well controlled (Scheme 1).[1,2] The power of Cu-ACA methodology is further heightened when the regioselectivity can be directed towards 1,6-adducts, thus opening the opportunity to deploy a subsequent 1,4-ACA on the reconjugated 1,6-adduct (Scheme 1, pathway A/B). Globally, the entire 1,6/1,4-ACA sequential process delivers enantio-enriched 1,3-dialkylated products in a straightforward manner circumventing the traditional iterative 1,4/1,4 process (Scheme 1, pathway C/D). However, despite the tactical advantage such a process could serve in target orientated synthesis, it has been seldom reported.[2d,2f,3]

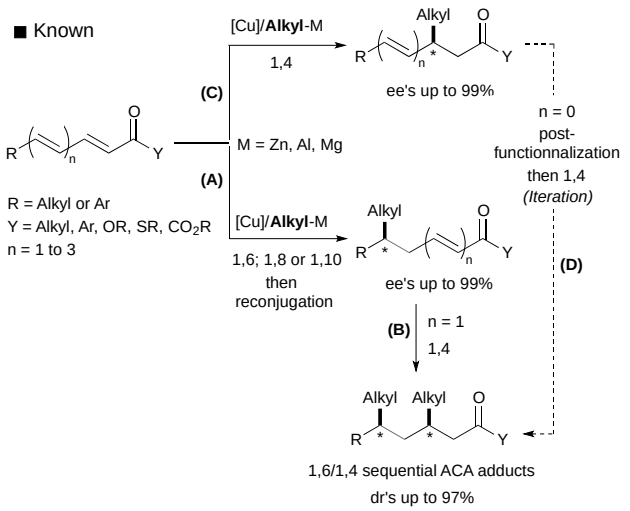

Scheme 1. Copper-catalyzed enantioselective conjugate addition of alkyl-metal hard nucleophiles to extended electron-deficient alkenes.

Minnaard, Feringa and co-workers reported in 2010 an efficient Cu/reversed Josiphos **L1** catalytic system for the 1,6-addition of

[a] C. Blons, T. Vives, Drs. M.S.T. Morin, T.E. Schmid, S. Colombel-Rouen, C. Crévisy, O. Baslé, M. Mauduit
Ecole Nationale Supérieure de Chimie de Rennes, CNRS, UMR 6226, 11 allée de Beaulieu, CS 50837, 35708 Rennes Cedex 7, France
E-mail: marc.mauduit@ensc-rennes.fr
[b] Drs. T. Reynaldo, J. Crassous
Université de Rennes 1, CNRS, UMR 6226, Campus de Beaulieu, 35042 Rennes Cedex, France.
[c] C.L. Covington, Prof. P.L. Polavarapu
Department of Chemistry, Vanderbilt University, Nashville, TN 37235, USA.
[d] Dr. S. Halbert, Prof. H. Gérard
Sorbonne Universités, UPMC Univ Paris 06, CNRS, Laboratoire de Chimie Théorique CC 137 - 4, place Jussieu F. 75252 Paris Cedex 05, France.
[e] S.N. Cuskelly, Profs. P.V. Bernhardt, Craig M. Williams
School of Chemistry and Molecular Biosciences, The University of Queensland, Brisbane, QLD 4072, Australia.

MeMgBr to dienic thioesters (Scheme 2-a).[2f] After reconjugation of the 1,6-adduct, a subsequent 1,4-ACA was performed on each enantiomer of the Josiphos ligand **L2** to give both the *syn*- and *anti*-1,3-dimethylated products; albeit in high stereoselectivities (up to 92% ee). Interestingly, after conversion of the thioester group of the *syn* adduct into an aldehyde and subsequent olefination, a second 1,6-ACA was attempted, which afforded (*syn*, *anti*) and (*syn*, *syn*) 1,3,5-trimethylated products with moderate and good diastereoselectivities, respectively. More recently, we reported the stereo-controlled introduction of two ethyl substituents having a 1,3-relationship, through a procedure involving a Cu/DiPPAM **L3** 1,6-ACA of Et_2Zn to linear aryldienones (up to 97% ee) followed by a reconjugation step, and a Cu/Binap **L4** catalyzed 1,4-ACA of Et_2Zn to the reconjugated 1,6-adduct (up to > 97% de) (Scheme 2-b).[2d]

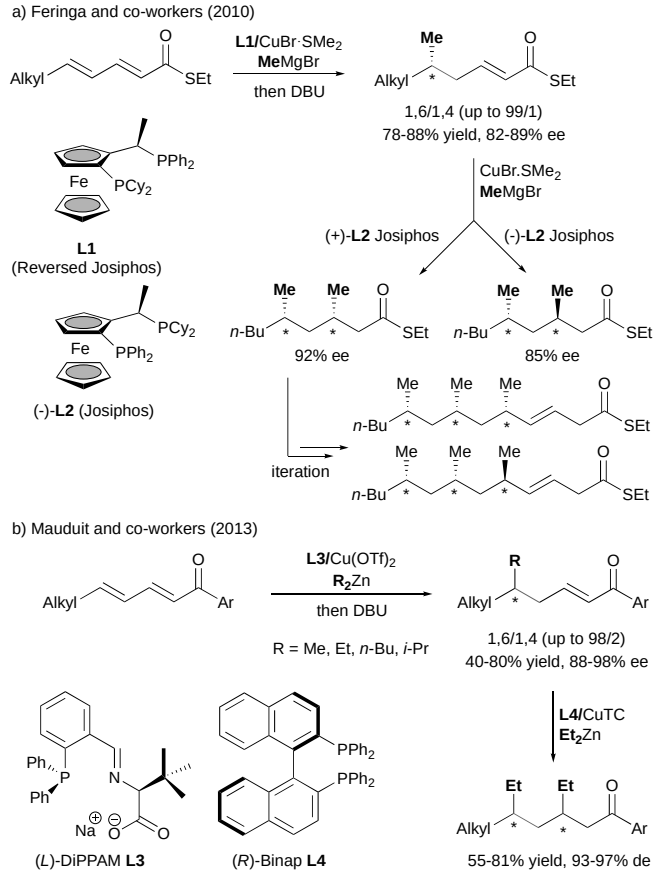

Scheme 2. First enantioselective sequential 1,6/1,4 Cu-catalyzed conjugate addition of C-metalated hard nucleophiles to acyclic dienic Michael acceptors and related iterative processes.

While all the examples presented above contain linear dienic conjugate acceptors, to the best of our knowledge, such a sequential process starting from 3-substituted cyclic dienones has only been reported on a single occasion. In 1978 Alexakis and Posner deployed this strategy during the synthesis of pseudoguaiane, but in the racemic series (Scheme 3).

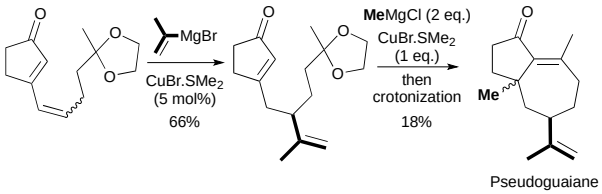

Scheme 3. Direct access to pseudoguaiane via a sequential 1,6/1,4 conjugate addition followed by an intramolecular cyclization as reported by Alexakis and Posner in 1978.

Nevertheless, some efficient catalytic systems were already described for copper-catalyzed 1,6-ACA of alkyl-metal nucleophiles to 3-substituted cyclohexenones.[2g,5] The first example was described by Alexakis and Mauduit in 2008.[2g] Using a chiral phosphoramidite as the ligand and Et_2Zn as the nucleophile, complete 1,6-regioselectivity and good ee (89%) were attained. More recently, DiPPAM **L3** and a variety of unsaturated hydroxyalkyl-NHCs, proved quite efficient for the Cu-catalyzed addition of various dialkylzincs to five- and six-membered cyclic dienones (ee's up to 99%).[5b-d] Considering these pioneering efforts, we envisioned that a sequential 1,6/1,4-ACA process applied to 3-substituted cyclohexenones, followed by a subsequent intramolecular cyclisation, could offer direct synthetic access to natural product scaffolds i.e. the drimane core **A** (Fig. 1). This bicyclic skeleton is present in many natural occurring biologically active molecules,[6] such as stachybotrylactam,[7] sclareolide[8] and coronarine E[9] (Fig. 1), but constitutes a real synthetic challenge. Besides obtaining control over the regio- and enantioselectivity of the sequential conjugate addition (including the formation of all-carbon quaternary centers),[10] the stereoselective intramolecular cyclisation via enolate trapping remains highly challenging. Indeed, although the tandem process consisting of a 1,4-ACA followed by intermolecular trapping of the enolate is very well documented,[11] the intramolecular version has been scarcely reported.[12]

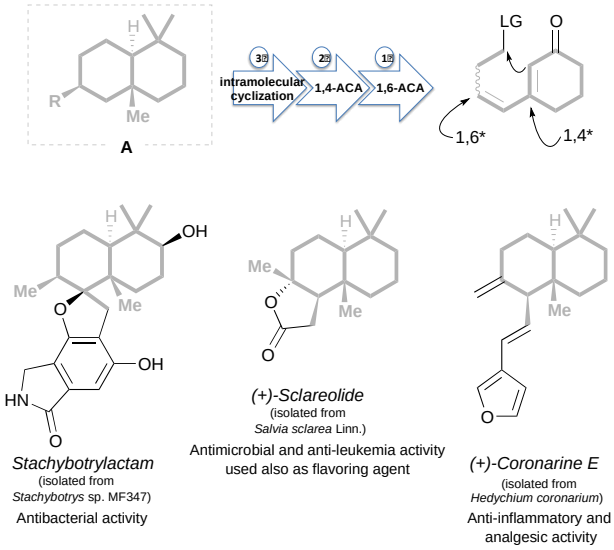

Figure 1. Top: Envisioned synthetic route to access the bicyclic core of various biologically active sesquiterpenes (Bottom).

We report herein the first stereoselective Cu-catalyzed sequential 1,6/1,4 ACA of carbon-metal nucleophiles to various 3-substituted cyclohexenones leading to enantio-enriched 1,3-dialkylated moieties. In addition, considering the relative flexibility of the lateral side chain, we developed a protocol to determine the absolute stereochemical configuration of the newly formed stereogenic centers utilising vibrational circular dichroism (VCD) and optical rotatory dispersion (ORD) analysis in combination with DFT calculations. Furthermore, a separate DFT study concerning the mechanism for C-C bond formation was undertaken to determine the origin of the 1,6-enantioselectivity. This highly stereoselective catalytic sequential process, in combination with the subsequent intramolecular cyclisation, was then applied to the synthesis of the challenging drimane skeleton.

Results and Discussion

1,6-ACA of diethylzinc to 3-substituted cyclohexenones catalysed by Cu(OTf)$_2$/(*L*)-DiPPAM L3

A set of 3-substituted cyclohexenones **S1**-**S5** was chosen to investigate the 1,6/1,4-ACA sequential process (Scheme 3). They differ in nature by the substituent at the delta position, and the configuration of the delta-gamma double bond. Substrates **S1**[2g] and **S2**[5d] bear an alkyl group, whereas **S3**-**S5** bear a functional group. The trialkylsilyloxy and the chloro substitutents were introduced in order to realize intramolecular trapping of the intermediate enolate formed in the 1,4-ACA, which would lead to the formation of the bicyclic skeleton (see Figure 1). Finally, the influence of the *E*/*Z* double bond configuration was probed with substrates **S3** and **S4**. Having the five dienones in hand (see ESI for details), we studied their behavior in the 1,6-ACA of diethylzinc catalysed by Cu(OTf)$_2$/(*L*)-DiPPAM **L3**. In a slightly modified procedure,[5c-d] 5 mol% of the copper source and 10 mol% of the ligand, were dissolved in THF before a 1 M solution of Et_2Zn in hexanes was added, followed by a solution of the dienone in THF. On reaction completion, the mixture was quenched with $NH_4Cl_{(s)}$ followed by the addition of a dichloromethane solution of DBU to initiate the reconjugation step. The results are summarized in scheme 4. In all cases, the desired 1,6-adducts were exclusively formed in moderate to good yields with excellent enantiomeric ratios ranging from 96.5:3.5 to 99:1. As expected, the involvement of the enantiomer of DiPPAM **L3** for dienone **S1**-**S2** led to the corresponding 1,6-products (-)-**P1** and (+)-**P2** having opposite configuration with a slight alteration of enantioselectivities (respectively 97:3 and 97.5:2.5 e.r.). Fortunately, regardless of the types of functional groups contained within dienones **S3**-**S5**, the catalytic system remained robust as corresponding 1,6-adducts **P3**-**P4** were obtained with similarly high enantioselectivities (96.5:3.5 to 97.5:2.5 e.r.); despite a lower isolated yield for **P3**. Interestingly, the enantiomeric outcome of the reaction is highly dependent on the configuration of the gamma-delta double bond, as **S3** and **S4** afforded opposite enantiomers. Such behaviour, which has recently been observed by Minnaard and Feringa in the copper catalysed 1,6-ACA of Grignard reagents to dienic esters,[2a] shows that isomerization of the double bond during the reaction does not occur to any significant extent.

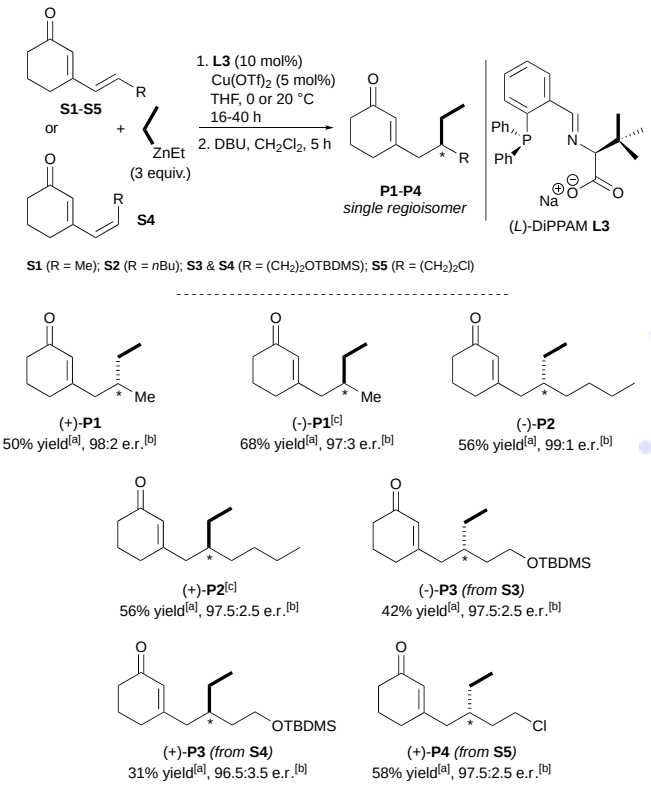

Scheme 4. Cu/DiPPAM **L3** catalyzed 1,6-ACA of diethylzinc to dienones **S1**-**S5**. [a] Isolated yields. [b] Determined by GC or HPLC on chiral columns. [c] (*D*)-DiPPAM [(*ent*)-**L3**] was used.

Before investigating the subsequent 1,4-ACA on **P1**-**P5** to build the targeted 1,3-dialkylated moieties, we decided to elucidate the absolute configuration of the 1,6-stereogenic center and determine the origin of the enantioselectivity promoted by our Cu(OTf)$_2$/(*L*)-DiPPAM **L3** catalytic system.

Vibrational Circular Dichroism (VCD) and optical rotatory dispersion (ORD) spectroscopy studies on the P1-adduct: determination of the absolute configuration

VCD spectroscopy[13-15] is a chiroptical technique operating in the infrared (IR) domain, which is useful for determining the absolute configuration (AC) of small molecules when other techniques fail [e.g. X-ray diffraction, electronic circular dichroism ECD)]. For example, due to issues with single crystals and the absence of chromophores, which is the case for most of the molecules described in this study. Like ECD the absolute configuration determination using VCD is achievable when the experimental VCD spectrum is directly compared to that calculated using DFT methods, provided that Boltzmann averaging is performed over all the accessible conformations. The experimental IR and VCD spectra were thus measured for **P1**, which displayed several bands in the 1000-1500 cm^{-1} region (Fig. 2).

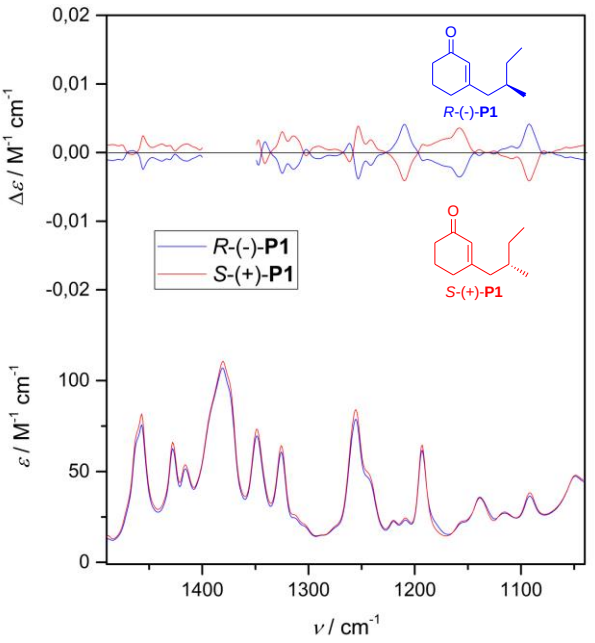

Figure 2. Experimental IR and VCD spectra of *R*-(–)- and *S*-(+)-**P1** measured in CD_2Cl_2. The VCD has been removed in the region where the solvent strongly absorbs.

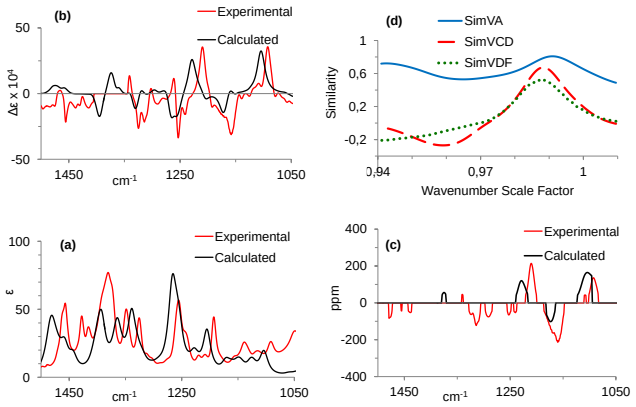

Figure 3. The VA (a), VCD (b), and VDF (c) spectra, with similarity analysis (d), for *R*-(–)-**P1**.

Considering the chirality of **P1** originates from only one asymmetric carbon, and due to the fact that the chiral exocyclic chain is quite flexible, the VCD signals of the (+) and (–) enantiomers were rather weak. **P1** enantiomers display mirror-image specific rotations values ($[\alpha]_D^{23}$ = -16.6 and +17.6 °·cm³·dm⁻¹·g⁻¹ in CH_2Cl_2, C = 0.016 and 0.019 g/100mL see ESI for specific rotations at other wavelengths). Nevertheless, with the aid of a thorough conformational analysis, both VCD spectra and specific rotation as a function of several wavelengths could be used to determine the *R*-(–) and *S*-(+) absolute configuration for **P1** using theoretical calculations, as described below. The conformational analysis was performed using the CONFLEX software package using the MMFF94s force field and a systematic search.[16] All conformations within 10 kcal/mol were re-optimized at the B3LYP/6-31G* level. For all conformations within a reasonable energy threshold, the structures were re-optimized at the B3LYP/Aug-cc-pVDZ level and VCD and ORD spectra were calculated at the same level of theory. All quantum chemical calculations were performed using GAUSSIAN 09.[17] In addition to VCD analysis, Vibrational Dissymmetry Factor (VDF) provided an additional level of confidence with the AC assignment.[18] For quantitative comparison between experiment and theory, similarity analysis was performed using the *'sim'* scoring functions,[19a] calculated using the the program CDSpecTech.[19b] *SimVCD* and *SimVDF* ratings can be used to assign the absolute configurations when used in conjunction with accurate visual comparison.[20] For *R*-(–)-**P1**, 22 unique conformations were found within 1.6 kcal/mol at the 6-31G* level, which constitutes ~94% of the Boltzmann weighted average (the lowest energy conformer is shown in Figure S1 of the ESI).

The vibrational absorption (VA), VCD, and VDF spectra for (–)-**P1** are shown in Figure 3, with similarity analysis comparing the (–)-enantiomer spectra with those predicted for *R* absolute configuration. The calculated spectra were Boltzmann weighted with Gibbs free energies. The peak similarity ratings obtained were 0.67 and 0.52 for *SimVCD* and *SimVDF* respectively, which are much larger than those needed for confident assignments.[18,19b,20a] The ORD calculations for the *R* configuration, shown in Fig. 4, match the experimental ORD for (–)-**P1.** Therefore, the AC of (–)-**P1** can be confirmed as *R*-(–), and (+)-**P1** as *S*-(+).

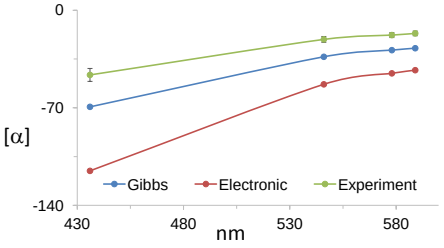

Figure 4. Comparison of the calculated and experimental ORD values for *R*-(–)-**P1**. The calculated SORs were Boltzmann weighted separately with electronic and Gibbs free energies.

Theoretical determination of enantioselectivity of 1,6-ACA catalyzed by Cu/DiPPAM: toward a rationale

Despite the positive experimental results, and the high selectivity of the Cu/DiPPAM **L3** catalyzed 1,6-ACA, little is known about the mechanistic aspects of this catalytic system.[21] We thus undertook a computational study (DFT calculations at B3PW91 and double zeta basis set with polarization, see Computational Details in ESI) of the pathway for formation of **P1** according to a mechanism proposed by Nakamura *et al.,*[22] and already successfully implemented in a recent study by our group.[21c] In this mechanism, the C-C bond formation step takes place in a bi-metallic species, herein called **A1** (Fig. 5 and ESI, Table S1, for detailed geometrical parameters). In this species, the exocyclic C=C bond of **S1** interacts through a π-bond with the Cu(I) center while one of the carbonyl lone pair is coordinated to the Zn center, which thus plays the role of a Lewis acid. In addition to that proposed by Nakamura, the DiPPAM ligand **L3** acts as a bridge between the two metal centers [Cu(Et) is coordinated to the

phosphine part while Zn(Et) interacts with the carboxylate arm of DiPPAM]. Coordination of the cyclic dienone in **A1** is well established with short Cu-C (2.029 Å – 2.172 Å) and Zn-O (2.111 Å) bond distances. Significant elongations with respect to the free ketone **S1** were observed for the C_5=C_6 (1.405 *vs* 1.344 Å) and C_2=O_1 (1.257 *vs* 1.223 Å) bonds, which is in line with significant activation of the substrate **S1**.

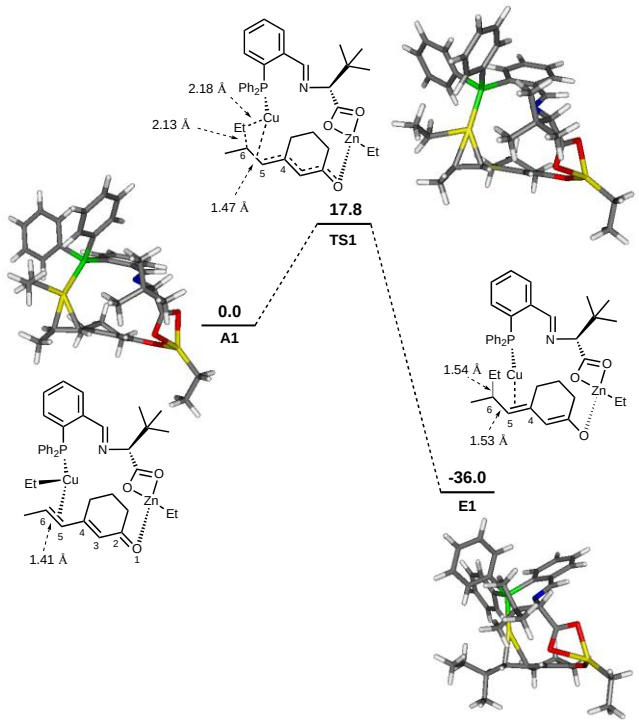

Figure 5. Gibbs free energy profile of the C-C bond formation step relative to the adduct **A1** (Gibbs Free Energy in kcal/mol and distances in Å).

The 1,6-conjugate addition proceeds through transition state **TS1** (Fig. 5 and ESI, Table S1, for detailed geometrical parameters). The C-C bond is formed on the C=C double bond side on which the Cu center was coordinated (*syn* addition). The activation barrier (in Gibbs Free Energy) is found to be 17.8 kcal.mol^{-1} whereas the formation of the zinc-enolate complex **E1** is exergonic by 36.0 kcal mol^{-1}. Following the Hammond postulate for exergonic reactions, the transition state is expected to be an "early" one and thus reactant-like. The geometrical properties of **TS1** are in agreement with this postulate, as the Cu···Et distance in **TS1** (2.182 Å) is near to the corresponding bond in **A1** (1.996 Å). Nevertheless, the forming C-C bond in **TS1** remains very long (2.125 Å), and thus far from the distance obtained in the enolate product **E1** (1.542 Å). It is thus possible to analyze the enantioselectivity of the reaction by examination of the potential arrangements of the ketone **S1** in the **A1** intermediate.[23]

We therefore explored various arrangements with intermediate **A1** taking into account i) the two possible conformations of the C_4-C_5 bond, ii) the two coordination faces of the substrate (pro-R and pro-S), iii) the two possible geometries of approach from the DIPPAM plane. This leads to eight possible structures (see Fig. 6). In order to properly represent steric and stacking effects, a dispersion correction was added to the DFT computations (B3PW91-D3, see Computational Details in ESI). Whereas in non-coordinated **S1**, the *S*-trans conformation of the C_4-C_5 bond was found to be favored by 2.2 kcal mol^{-1} this preference is not conserved in the adduct **A1.** The *S*-cis structures [(e) to (h) in Fig. 6)] are all more stable than their *S*-trans counterparts. The most stable arrangement found [structure (g)] is associated with the formation of the *S*-isomer, in full agreement with the VCD results. It is believed that this conformation is stabilized by a complex network of CH-π interactions. For instance, one interaction is observed between the *t*-Bu group and a phenyl group of the diphenylphosphino moiety. Another interaction involves the CH_2 of the cyclohexenone core and the phenyl group attached to the imino group.

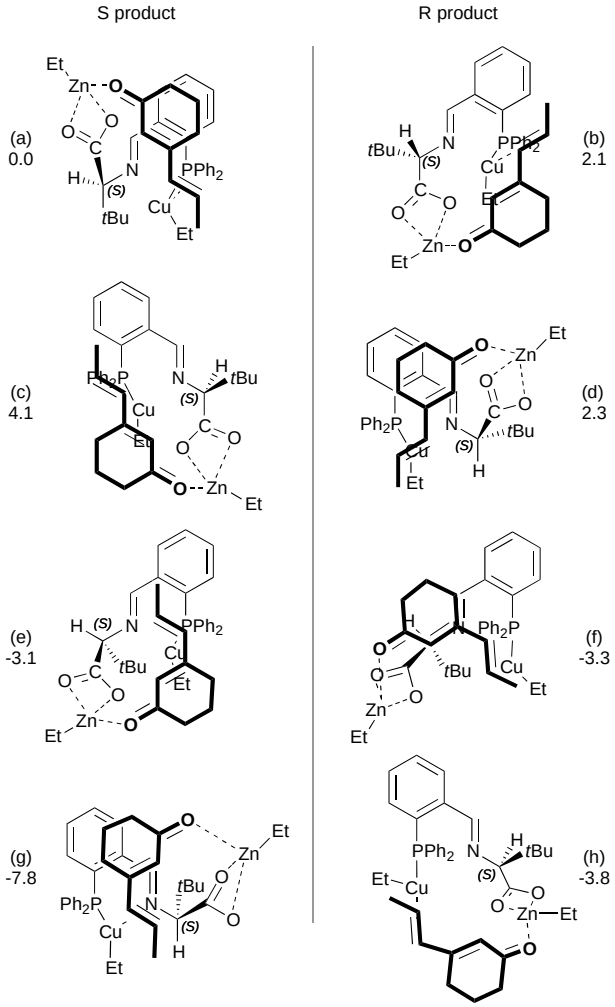

Figure 6. Eight possible structures computed for **A1** with S-DIPPAM **L3** and cyclic dienone **S1** in the *S*-trans or *S*-cis conformation at the terminal C=C double bond. Structures on the left yield the *S* enantiomer and those on the right lead to the *R*. Energies with respect to structure (a) (referred as 0.0) are provided.

Confirmation of the AC by X-ray analysis

When (+)-P3 underwent deprotection to reveal the OH function for conversion into a leaving group, we observed an undesired, but ultimately fortuitous intramolecular 1,4-addition of the OH group at the beta-carbon. This led to the formation of two diastereoisomeric spiro compounds **SPa** and **SPb** which were isolated in moderate yields (resp. 30% and 33%) after column chromatography

(Scheme 5). Fortunately, crystals could be obtained for **SPa** and from X-ray analysis the configuration was determined as 4*S*, 6*R*. Consequently, it was confirmed that (+)-**P3** had *R* stereochemistry. In the view that (+)-**P3** was obtained from a Cu/(L)-DiPPAM catalyzed 1,6-ACA involving a (*Z*)-dienone, this outcome is in complete agreement with the above VCD/ORD results and theoretical calculations.

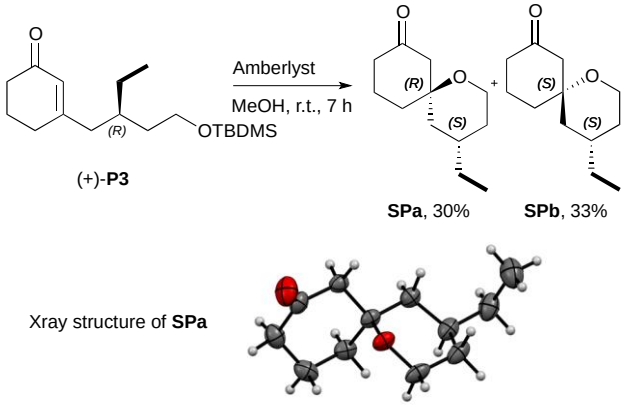

Scheme 5. Synthesis of spiro compounds **SPa** and **SPb**; thermal ellipsoid plot generated with Mercury v3.8 (http://www.ccdc.cam.ac.uk/mercury/) showing the X-ray crystal structure of **SPa** with 30% probability ellipsoids.

Subsequent Cu-catalyzed 1,4-ACA of methyl derived hard nucleophiles: formation of the all-carbon quaternary centers

Having successfully developed a 1,6-ACA reaction with various cyclic dienones a search was initiated for a desirable combination of catalytic system and organometallic nucleophile, which would provide the optimum 1,4-regio- and enantioselectivity. As depicted in Figure 7 and scheme 6, two families of chiral ligands were evaluated (hydroxyalkyl-NHCs **L5**-**L6**, and phosphoramidites **L7**-**L9**) along with 2 types of methyl nucleophiles (Grignard reagents and trialkylaluminums).

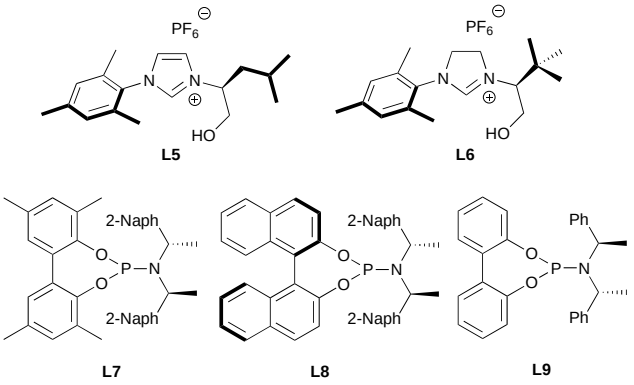

Figure 7. Screened Ligands **L5**-**L9** for the 1,4-ACA addition of 3-substituted cyclohexenones.

Furthermore, it was anticipated that the presence of a bulky (branched) substituent at the beta-position of **P1**-**P4** would make it more difficult to procure the 1,4-ACA step as compared to those already described in the literature. Therefore, it was decided to perform a preliminary study with a simplified substrate **S6** bearing an isobutyl group; a similar feature to **P1**-**P4** (Scheme 5). Under experimental conditions close to those already described, or adapted from the literature,[5b,10k,24] the expected 1,4-adduct **P9** was formed with significant differences in both yield and enantio-induction. Curiously, although hydroxyalkyl-NHCs **L5**-**L6** usually give good results in Cu-ACA, notably in the formation of all-carbon quaternary centers,[10e,k,m] they were found to be quite inefficient toward **S6** (i.e. irrespective of the nucleophilic source investigated noticeable amounts of undesired 1,2-adducts **P9b** were observed, see ESI for details). A maximum of 24% yield and 52% ee were reached with MeMgBr. An improved yield was observed with $AlMe_3$, but with a significantly lower e.r. of 54.5:45.5. Phosphoramidite ligands **L7**-**L8** appeared more appropriate in combination with $AlMe_3$, and in turn surpassed **L5**-**L6** both in terms of stereoselectivities and yields. The highest result was gained with **L7**/$(CuOTf)_2{\cdot}C_6H_6$ (83% yield and 98.5:1.5 e.r.).

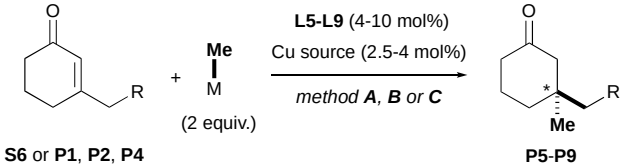

S6 (R = *i*Pr); **P1** (R = *CH(Et)Me); **P2** (R = *CH(Et)*n*Bu)
P4 (R = *CH(Et)CH_2CH_2Cl)

*Method **A**:* $Cu(OTf)_2$ (3 mol%), **L5** or **L6** (4 mol%), Et_2O, 0 °C, 2 h.
*Method **B**:* $Cu(OTf)_2$ (4 mol%), **L5** (6 mol%), *n*BuLi (16 mol%), THF, rt, 2.5 h.
*Method **C**:* $(CuOTf)_2.C_6H_6$ (2.5 mol%), **L7**-**L9** (10 mol%), Et_2O, -10 °C, 14 h.

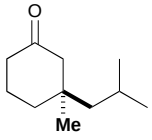

(+)-**P9** *(from **S6**)*

With **L6**/MeMgBr *(method **A**)*: 24% yield[a,b], 76:24 e.r.[c]
L5/$AlMe_3$ *(method **B**)*: 58% yield[a,d], 54.5:45.5 e.r.[c]
L7/$AlMe_3$ *(method **C**)*: 83% yield[a], 98.5:1.5 e.r.[c](*R*)[e]
L8/$AlMe_3$ *(method **C**)*: 50% yield[a], 97.5:2.5 e.r.[c]

With **L7**/$AlMe_3$: *(method **C**)*

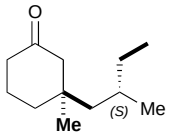

(+)-**P5** *(from (+)-**P1**)*
81% yield[f], 99:1 d.r.[g]

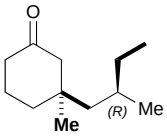

(-)-**P6** *(from (-)-**P1**)*
57% yield[f], 99:1 d.r.[g]

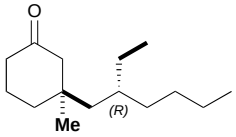

(-)-**P7** *(from (-)-**P2**)*
75% yield[f], 98.5:1.5 d.r.[g]

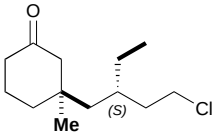

(-)-**P8** *(from (+)-**P4**)*
56% yield[f], 98.5:1.5 d.r.[g]

With **L9**/$AlMe_3$: *(method **C**)*

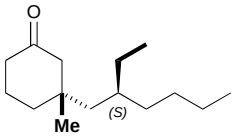

(+)-**P7** *(from (+)-**P2**)*
66% yield[f], 89.5:10.5 d.r.[g]

Scheme 6. Cu-catalyzed 1,4-ACA of MeMgBr or $AlMe_3$ to 3-substituted cyclohexenones with ligands **L5**-**L9**. [a] NMR yields. [b] 37% of 1,2-adduct **P9b** were also formed. [c] The enantiomeric ratio was determined by GC on chiral columns. [d] 11% of 1,2-adduct **P9b** were also formed. [e] The absolute configuration (*R*) was assigned in accordance with previous results reported by Alexakis.[12b] [f] Isolated yield. [g] The diastereomeric ratio was determined by GC on chiral phase columns.

Furthermore, the same level of selectivity was reached when $AlEt_3$ was utilised as the nucleophile (99:1 e.r., see ESI for details). As the combination of the Cu/phosphoramidite catalytic system with trialkylaluminum appeared the most efficient for the 1,4-ACA of sterically congested 3-substituted cyclohexenones, more challenging substrates were evaluated (i.e. **P1**, **P2** and **P4**) (Scheme 6). When the reaction was carried out with **L7**/$(CuOTf)_2{\cdot}C_6H_6$, the expected products **P5**, **P6**, (–)-**P7** and **P8** were all isolated in good to high yields (57-81%) and excellent diastereoisomeric ratios (98.5:1.5 to 99:1). However, when phosphoramidite **L9** was deployed in order to obtain (+)-**P7**, the 1,4-adduct was formed with a lower stereoselectivity (89.5:10.5 e.r.).[24]

VCD spectroscopy studies on P5, P6 and P7 adducts: determination of the absolute configuration.

The relative configurations of **P5**, **P6** and **P7** were also investigated by chiroptical spectroscopy. The experimental IR and VCD of **P5** and **P6** diastereomers were measured and are depicted in Figure 8. Although they have a diastereomeric relationship that encompasses two asymmetric C^3 and $C^{2'}$ carbons, they possess the same IR spectrum and very similar VCD signals [especially the bisignate peaks around 1300 cm^{-1} and 1200 cm^{-1} corresponding to CCH bending modes within the cycle (see ESI)]. Comparison with theoretical calculations (*vide infra*) showed that these two signals arise from the *R* stereochemistry at the C^3 carbon. In addition, **P5** and **P6** respectively result from the asymmetric addition of *S*-(+) and *R*-(–)-**P1** (i.e. their configuration at $C^{2'}$ is retained). At this stage it is worth noting that this stereochemical assignment (i.e. 3*R*,2'*S*-(+)-**P5**, 3*R*,2'*R*-(–)-**P6**) is in total accord with the result obtained by Alexakis et *al*.[24a]

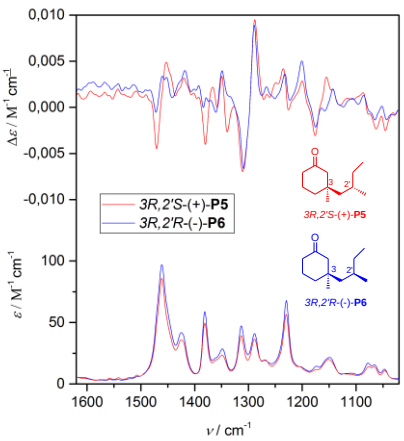

Figure 8. Experimental IR and VCD spectra of 3*R*,2'*S*-(+)-**P5** and 3*R*,2'*R*-(–)-**P6** measured in CD_2Cl_2.

Conformational analysis proceeded using the methods outlined above, except all conformations were optimized at the PM6 level before proceeding to DFT methods. This additional optimization was undertaken to reduce the number of conformations. For the (3*R*,2'*S*) diastereomer, all conformations within 3.1 kcal/mol (85 total) were retained at the PM6 level, then 18 conformations were found within 2 kcal/mol at B3LYP/Aug-cc-pVDZ level and were used for VCD and ORD calculations (the lowest energy conformers determined with Gibbs free energies are shown in Figure S2 of ESI).

For the (3*R*,2'*R*) diastereomer all conformations within 3.0 kcal/mol (83 total) were retained at the PM6 level, then 18 conformations were found within 2 kcal/mol at B3LYP/Aug-cc-pVDZ level and were used for VCD and ORD calculations. The experimental VA, VCD, and VDF spectra for both diastereomers (**P5** and **P6**) and the corresponding calculated spectra for (3*R*,2'*R*) and (3*R*,2'*S*) diastereomers are shown in Figure 9. Visual comparison of the calculations reveals that the majority of the VCD features have the same sign, and though there are some differences in some band magnitudes, determination of the relative configuration cannot be made from VCD alone. VDF comparison seemed to provide more discriminating power for the 1350 cm^{-1} band, suggesting a correlation between **P5** and the (3*R*,2'*S*) diastereomer, with additional support from the positive band at 1200 cm^{-1}. Though VCD and VDF analysis would suggest that the (3*R*,2'S) configuration can be assigned to **P5**, the assignment based on only one chiroptical method is not normally advised,[25] especially when diastereomers exhibit similar spectra. In the present case, even though the AC at the 2' position may be fixed from that of the precursor, it is always recommended to confirm the relative configuration with other methods whenever possible.

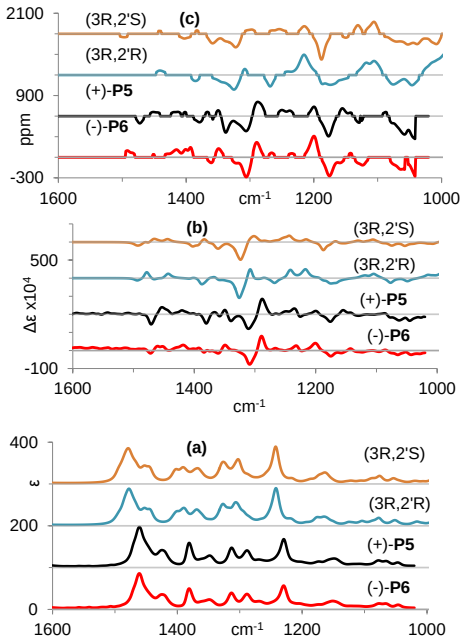

Figure 9. The experimental VA (a), VCD (b), and VDF (c) spectra of **P5** and **P6** and the corresponding calculated spectra for (3*R*,2'*S*) and (3*R*,2'*R*) diastereomers.

The comparison of calculated and experimental optical rotatory dispersion (ORD) curves provides another means of analysis and can elevate confidence with the assignment of diastereomers. ORD curves for **P5** and **P6** are shown in Figure 10. DFT calculations predict a change in the sign of the ORD for the (3*R*,2'*S*) configuration from positive at long wavelengths to negative at shorter wavelengths, and this is seen in the experimental ORD only for (+)-**P5**. The (3*R*,2'*R*) configuration is predicted to have negative values of ORD in the 600-400 nm region with increasing magnitudes at shorter wavelengths, and

this is indeed observed experimentally for (-)-**P6**.

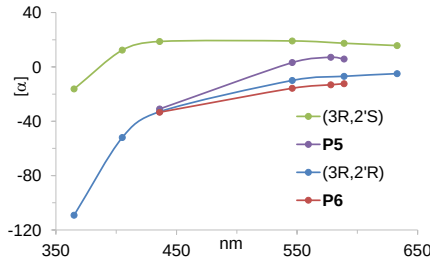

Figure 10. The theoretical and experimental ORD for **P5** and **P6** and calculated ORD for (3*R*,2'*S*) and (3*R*,2'*R*) diastereomers.

This trend in configurational assignments matched that found from VCD analysis, and therefore the AC and relative configuration of both diastereomers were confidently assigned. Also this outcome confirmed the AC at the 3 position to be the *R*-configuration, and confirmed that the stereochemistry of the 2' position is retained from the precursor (+)-**P1** and (–)-**P1**. Finally, the experimental IR and VCD spectra of (+)- and (–)-**P7** were measured and are depicted in Figure 11. Here again, two asymmetric C^3 and $C^{2'}$ carbons are present. Overall, sample (+)- and (–)-**P7** have an enantiomeric relationship, but they present different enantiomeric and diastereomeric purities (see Table S2 in ESI). Overall, they displayed similar IR spectra and mirror-image VCD signals. The clear bisignate signatures around 1300 cm^{-1} and 1200 cm^{-1} that were also found in **P5** and **P6**, easily enabled assignment of the 3*S*-(+) and 3*R*-(-)-**P7** absolute configuration by simple comparison. This result is in total agreement with Alexakis' results[24a] (*vide supra*). However, due to the huge number of conformations accessible to the pendant chain, the VCD calculations are prohibitive and do not enable absolute configuration to be assigned clearly at the $C^{2'}$ atom. The absolute configurations of other ACA products were further assigned by analogy with the configurations of **P1**, **P5**, **P6** and **P7** determined by VCD studies (see ESI).

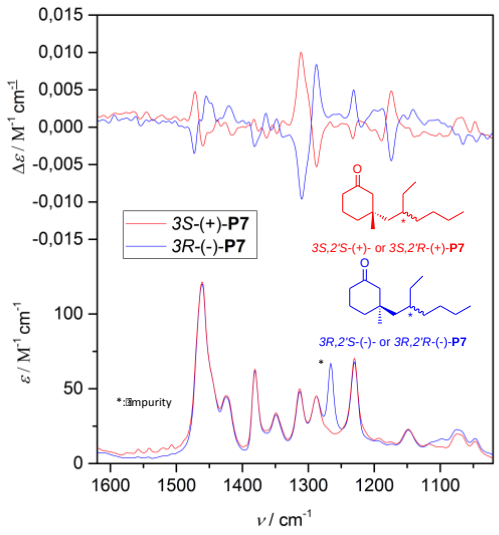

Figure 11. Experimental IR and VCD spectra of *R*-(–)- and *S*-(+)-**P7** measured in CD_2Cl_2.

Subsequent intramolecular cyclization : towards the formation of the drimane skeleton

Having successfully formed the all-carbon quaternary stereogenic center at the 1,4-position on **P1**, **P2** and **P4**, the intramolecular cyclisation leading to the highly desired bicyclic drimane skeleton was pursued (Scheme 7). Unfortunately, even starting from the (+)-**P4** 1,6-adduct bearing the chloro leaving group, failed to deliver the bicyclic product **P10** (Scheme 6, conditions A). On acidic work up (NH_4Cl) the 1,4-adduct (–)-**P8** was isolated in 72% yield. This was not surprising since aluminum enolates are known to be less reactive.[11c,26] Conversion of the Al enolate into the corresponding ate-complex with MeLi, and addition of HMPA (Scheme 6, conditions B), did not improve reactivity unfortunately (i.e. cyclized product **P10** was not detected).[26,27] As the tandem 1,4-ACA/enolate trapping appeared difficult to realize, it was decided to perform the cyclization starting from isolated **P8**, following a procedure already described on similar substrates.[10d,28] In the presence of KH, chloro-ketone **P8** was easily converted into **P10**, which was isolated in a 93% overall yield (d.r. 1:1). Hopefully, diastereoisomers **10a** and **10b** could be readily separated in 44% and 33% yields, respectively. **P10b**, having the *trans*-fused bicycle (see ESI for details), now sets the stage for others pursing this class of natural product, where geminal dimethylation of the carbonyl would play a critical role.[29]

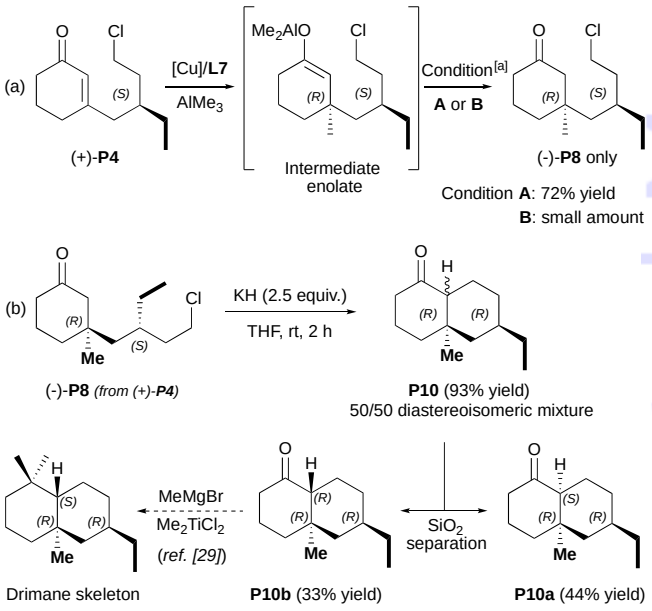

Scheme 7. Formation of the bicyclic product **P10**, a direct precursor of the drimane core: (a) via 1,4-ACA/intramolecular enolate trapping sequence from (+)-**P4** and (b) via intramolecular cyclisation from (-)-**P8** adduct. [a] Condition **A**: room temperature, 16 h, NH_4Cl; Condition **B**: Concentration; then HMPA, MeLi (1.4 equiv.), rt, 24 h; then NH_4Cl.

Conclusions

To conclude, the first stereocontrolled Cu-catalyzed sequential 1,6/1,4-conjugate addition of alkyl-metal nucleophiles to cyclic dienones has been reported. Various dienones were evaluated using a Cu/DiPPAM catalytic system and Et_2Zn as the nucleophile, which afforded the expected product in high ee's (up to 98%) after the reconjugation step. A Cu/phosphoramidite catalytic system utilising trialkylaluminum reagents proved to be

the most efficient combination for the subsequent 1,4-ACA, which led to the 1,3-dialkylated products, comprising an all-carbon quaternary center, with excellent de's (up to 98%). In addition, despite the relative flexibility of the exocyclic chain, the absolute stereochemical configuration was established through vibrational circular dichroism (VCD) and optical rotatory dispersion (ORD) analysis in combination with DFT calculations. Furthermore, the mechanism for the 1,6-addition was addressed through DFT calculations and the proposed catalytic intermediate determined to be a bimetallic complex, in which Zn ensures the docking of the carbonyl function and Cu controls the facial selectivity, and thus the enantioselectivity via a π-interaction. The experimental results were found to be fully compatible with the theoretically proposed mechanism and have been confirmed by X-Ray analysis of a functionalized 1,6-ACA adduct. Lastly, this highly stereoselective catalytic sequential process in combination with a subsequent intramolecular cyclisation was then successfully applied to the enantioselective synthesis of the challenging drimane core skeleton.

Experimental Section

General experimental procedure for $Cu(OTf)_2$/DiPPAM L3 catalyzed 1,6-ACA on dienones S1-S5. A flame dried Schlenk, under an argon atmosphere, was charged with DiPPAM ligand **L3** (21.3 mg, 0.05 mmol, 10 mol%), $Cu(OTf)_2$ (9.0 mg, 0.025 mmol, 5 mol%) and anhydrous THF (1 mL). The resulting mixture was stirred for 10 min. A 1 M solution of diethylzinc in hexanes (1.5 mL, 1.5 mmol, 3 equiv.) was added and the reaction mixture was stirred for 10 min. Finally, a solution of substrate (0.5 mmol, 1 equiv.) in 0.5 mL of THF was added. The reaction mixture was stirred for 16-40 h at the required temperature. The reaction was quenched by the addition of solid NH_4Cl (500 mg) and the mixture was stirred for 1h. Then, anhydrous CH_2Cl_2 (4 mL) and DBU (100 µL, 0.7 mmol, 1.4 equiv.) were added. The mixture was stirred for 5 h. The solution was filtered on a small pad of silica, washed with EtOAc, and concentrated under vacuo. The crude product was purified by flash chromatography on silica gel (pentane/Et_2O 85/15 for **P1** and **P2**, pentane/Et_2O 90/10 to 85/15 for **P3**, pentane/Et_2O 80/20 to 60/40 for **P4**). The enantiomeric excess was determined by GC or HPLC analysis of the purified compound.

General experimental procedure for $(CuOTf)_2{\cdot}C_6H_6$/L7 catalyzed 1,4-ACA on enones (+)-P1, (-)-P1, (+)-P2, (-)-P2, (+)-P4. A flame-dried Schlenk tube was charged with $(CuOTf)_2{\cdot}C_6H_6$ (6.3 mg, 2.5 mol%) and the chiral phosphoramidite **L7** (29.8 mg, 10 mol%). Anhydrous Et_2O (1 mL) was added and the mixture was stirred at room temperature for 30 min. Then the Michael acceptor (1.0 equiv., 0.5 mmol) in Et_2O (1 mL) was added dropwise at room temperature and the reaction mixture was stirred for further 5 min before being cooled to -10 °C. Then, trimethylaluminum (0.5 mL of 2 M solution in hexanes, 2.0 equiv.) was introduced dropwise. Once the addition was complete the reaction mixture was left at -10 °C for 14 h. The reaction was hydrolyzed by the addition of solid NH_4Cl (500 mg) at -10 °C, and stirred for 1 h at rt. The solution was filtered on a pad of silica gel, washed with EtOAc, and concentrated in vacuo. GC analysis was performed on the crude product to determine the diastereomeric excess. The oily residue was purified by flash column chromatography to yield the 1,4-adduct (pentane/Et_2O 97/3 to 90/10 for **P5** and **P6**, toluene/Et_2O, 97/3 for **P7** or pentane/Et_2O 90/10 to 80/20 for **P8**). The enantiomeric excess was determined by GC or HPLC analysis of the purified compound.

Acknowledgements

MSTM, SH, HG, CC and MM thank the Agence Nationale de la Recherche (SCATE project: ANR-12-BS07-0009-01) for financial support. MM thanks Pr A. Alexakis for generous gift of phosphoramidite ligands. MM and CC thank J.-P. Guégan for his contribution to NMR deconvolution studies related to 1,4-ACA experiments to enone **S6** and elucidation of **P10** diastereoisomers. CLC and PLP thank the NSF (CHE-0804301) for financial support. This work was conducted in part using the resources of the Advanced Computing Center for Research and Education (ACCRE) at Vanderbilt University, Nashville, TN. J.C. acknowledges the ANR (10-BLAN-724-1-NCPCHEM). CMW, PVB and SNC gratefully acknowledge the University of Queensland for financial support, and the Australian Research Council (ARC) for a Future Fellowship award (FT110100851) to CMW

Keywords: Asymmetric catalysis • copper • conjugate addition • VCD/ORD • absolute configuration

[1] For general reviews dealing with ACA to extended Michael acceptors, see: (*a*) Metal catalyzed Asymmetric nucleophilic addition to electron-deficient alkenes M. Mauduit O. Baslé, H. Clavier, C. Crévisy, A. Denicourt-Nowicki, in *Comprehensive Organic Synthesis II*, Vol. 4 (Eds.: G. A. Molander, P. Knochel), Elsevier, **2014**, pp. 189; (*b*) E. M. P. Silva, A. M. S. Silva, *Synthesis*, **2012**, *44*, 3109; (*c*) A. G. Csákÿ, G. de la Herrán, M. C. Murcia, *Chem. Soc. Rev*. **2010**, *39*, 4080.

[2] For selected papers dealing with the regiocontrol of metal-catalyzed ACA to dienic and polyenic substrates, see: (*a*) T. den Hartog, Y. Huang, M. Fañanás-Mastral, A. Mauwese, A. Rudolph, M. Pérez, A. J. Minnaard, B. L. Feringa, *ACS Catal*., **2015**, *5*, 560; (*b*) J. Lu, J. Ye, and W.-L. Duan, *Chem. Commun*., **2014**, *50*, 698; (*c*) Z. Ma, F. Xie, H. Yu, Y. Zhang, X. Wu, W. Zhang, *Chem. Commun*., **2013**, *49*, 5292; (*d*) M. Magrez-Chiquet, M. S. T. Morin, J. Wencel-Delord, S. Drissi Amraoui, O. Baslé, A. Alexakis, C. Crévisy, M. Mauduit, *Chem. Eur. J.*, **2013**, *19*, 13663; (*e*) M. Tissot, D. Poggiali, H. Hénon, D. Müller, L; Guénée, M. Mauduit, A. Alexakis, *Chem. Eur. J.*, **2012**, *18*, 8731; (*f*) T. den Hartog, D. J. van Dijken, A. J. Minnaard, B. L. Feringa *Tetrahedron: Asymmetry*, **2010**, *21*, 1574; (*g*) H. Hénon, M. Mauduit, A. Alexakis, *Angew. Chem. Int. Ed.*, **2008**, *47*, 9122; (*i*) T. den Hartog, S. R. Harutyunyan, D. Font, A. J. Minnaard, B. L. Feringa*, Angew. Chem. Int. Ed*., **2008**, *47*, 398.

[3] For an example of Ir/Rh-catalysed sequential 1,6/1,4-ACA, see: T. Nishimura, Y. Yasuhara, T. Sawano, T. Hayashi, *J. Am. Chem. Soc*., **2010**, *132*, 7872.

[4] A. Alexakis, M. J. Chapdelaine, G. H. Posner, A. W. Runquist, *Tetrahedron Lett.*, **1978**, *44*, 4205.

[5] (*a*) M. S. T. Morin, T. Vives, O. Baslé, C. Crévisy, V. Ratovelomanana-Vidal, M. Mauduit, *Synthesis*, **2015**, *47*, 2570; (*b*) C. Jahier-Diallo, M. S. T. Morin, P. Queval, M. Rouen, I. Artur, P. Querard, L. Toupet, C. Crévisy, O. Baslé, M. Mauduit, *Chem. Eur. J.*, **2015**, *21*, 993; (c) M. Magrez, J. Wencel-Delord, A. Alexakis, C. Crévisy, M. Mauduit, *Org. Lett*., **2012**, *14*, 3576. (*d*) J. Wencel-Delord, A. Alexakis, C. Crévisy, M. Mauduit, *Org. Lett.* **2010**, *12*, 4335; For an example involving Rh- and Ir-complexes, see: (*e*) T. Nishimura, A. Noishiki, T. Hayashi, *Chem. Commun*., **2012**, *48*, 973; (*f*) T. Hayashi, S. Yamamoto, N. Tokunaga, *Angew. Chem. Int. Ed*., **2005**, *44*, 4224; (g) T. Hayashi, N. Tokunaga, K. Inoue, *Org. Lett.* **2004**, *6*, 305.

[6] For a review on occurrence, biological activity and synthesis of drimane sesquiterpenoids, see : N. J. M. Jansen, Ae. de Groot, *Nat. Prod. Res*., **2004**, *21*, 449.

[7] B. Wu, V. Oesker, J. Wiese, S. Malien, R. Schmaljohann, J. F. Imhoff, *Mar. Drugs*, **2014**, *12*, 1924.

[8] K. Dimas, D. Kokkinopoulos, C. Demetzos, B. Vaos, M. Marselos, M. Malamas, T. Tzavaras, *Leukemia Research*, **1999**, *23*, 217.

[9] (a) M. Jung, I. Ko, S. Lee, *J. Nat. Prod*., **1998**, *61*, 1394. (b) M. Müller, J. Schröder, C. Magg, K. Seifert, *Tetrahedron Lett.*, **1998**, *39*, 4655.

[10] For an excellent review dealing with the 1,4-ACA of 3-substitued cyclic enones, see: (*a*) C. Hawner, A. Alexakis, *Chem. Commun*., **2010**, *46*, 7295. For a selection of recent papers, see: (*b*) M. Sidera, P. M. C Roth, R. M. Maksymowicz, S. P. Fletcher, *Angew. Chem. Int. Ed*. **2013**, *52*, 7995; (*c*) D. Müller, A. Alexakis, *Chem. Eur. J*., 2013, **19**, 15226; (*d*) D. Müller, A. Alexakis, *Org. Lett.*, **2013**, *15*, 1594; (*e*) N. Germain, M. Magrez, S. Kehrli, M. Mauduit, A. Alexakis, *Eur. J. Org. Chem*. **2012**, 5301; (*f*) K. Kikushima, J. C. Holder, M. Gatti, B. M. Stoltz, *J. Am. Chem. Soc*., **2011**, *133*, 6902; (*g*) T. L. May, J. A. Dabrowski, A. H. Hoveyda, *J. Am. Chem. Soc*., **2011**, *133*, 736; (*h*) D. Müller, M. Tissot, A. Alexakis, *Org. Lett.* **2011**, *13*, 3040; (*i*) C. Hawner, D. Müller, L. Gremaud, A. Felouat, S. Woodward, A. Alexakis, *Angew. Chem. Int. Ed*., **2010**, *49*, 7769; (*j*) R. Shintani, M. Takeda, T. Nishimura, T. Hayashi, *Angew. Chem. Int. Ed*., **2010**, *49*, 3969; (*k*) S. Kehrli, D. Martin, D. Rix, M. Mauduit, A. Alexakis, *Chem. Eur. J*., **2010**, *16*, 9890; (*l*) D. Müller, C. Hawner, M. Tissot, L. Palais, A. Alexakis, *Synlett*, **2010**, 1694; (m) D. Martin, S. Kerhli, M. d'Augustin, H. Clavier, M. Mauduit, A. Alexakis, *J. Am. Chem. Soc*., **2006**, *133*, 736

[11] For reviews dealing with the tandem copper catalyzed 1,4-ACA of organometallic reagents/enolate trapping, see : (*a*) Z. Galeštoková, R. Šebesta, *Eur. J. Org. Chem*., **2012**, 6688; (*b*) T. Jerphagnon, M. G. Pizzuti, A. J. Minnaard, B. L. Feringa, *Chem. Soc. Rev*. **2009**, *38*, 1039. For selected recent papers: (*c*) N. Germain, A. Alexakis, *Chem. Eur. J.*, **2015**, *21*, 8597; (*d*) Z. Sorádová, J. Máziková, M. Mečiarová, R. Šebesta, *Tetrahedron: Asymmetry*, **2015**, *26*, 271; (*e*) B. C. Calvo, A. V. R. Madduri, S. R. Harutyunyan, A. J. Minnaard, *Adv. Synth. Catal*., **2014**, *356*, 2061; (*f*) N. Germain, D. Schlaefli, M. Chellat, S. Rosset, A. Alexakis, *Org. Lett*., **2014**, *16*, 2006; (*g*) N. Germain, L. Guénée, M. Mauduit, A. Alexakis, *Org. Lett.*, **2014**, *16*, 118; (*h*) C. Bleschke, M. Tissot, D. Müller, A. Alexakis, *Org. Lett*., **2013**, *15*, 2152; (*i*) M. Welker, S. Woodward, A. Alexakis, *Org. Lett.*, **2010**, *12*, 576. See also ref 10k.

[12] (*a*) T. den Hartog, A. Rudolph, B. Maciá, A. J. Minnaard and B. L. Feringa, *J. Am. Chem. Soc*., 2010, **132**, 14349; (*b*) K. Li and A. Alexakis, Chem. Eur. J., 2007, **13**, 3765.

[13] L. A. Nafie in *Vibrational Optical Activity: Principles and Applications*. Wiley-VCH, New York, **2011**.

[14] L. A. Nafie Infrared Vibrational Optical Activity: Measurement and Instrumentation. in *Comprehensive Chiroptical Spectroscopy*, *Vol. 1*, Wiley-VCH, New York, **2012**, pp 115.

[15] L. D. Barron in *Molecular Light Scattering and Optical Activity*. Cambridge Univ. Press, Cambridge, UK, 2nd edition, **2009**.

[16] Conflex Program, CONFLEX Corporation, AIOS Meguro 6F, 2-15-19, Kami-Osaki, Shinagawa-Ku, Tokio 141-0021, Japan; www.conflex.us.

[17] M. J. Frisch, G. W. Trucks, H. B. Schlegel, G. E. Scuseria, M. A. Robb, J. R. Cheeseman, G. Scalmani, V. Barone, B. Mennucci, G. A. Petersson, H. Nakatsuji, M. Caricato, X. Li, H. P. Hratchian, A. F. Izmaylov, J. Bloino, G. Zheng, J. L. Sonnenberg, M. Hada, M. Ehara, K. Toyota, R. Fukuda, J. Hasegawa, M. Ishida, T. Nakajima, Y. Honda, O. Kitao, H. Nakai, T. Vreven, J. A., Jr. Montgomery, J. E. Peralta, F. Ogliaro, M. Bearpark, J. J. Heyd, E. Brothers, K. N. Kudin, V. N. Staroverov, R. Kobayashi, J. Normand, K. Raghavachari, A. Rendell, J. C. Burant, S. S. Iyengar, J. Tomasi, M. Cossi, N. Rega, N. J. Millam, M. Klene, J. E. Knox, J. B. Cross, V. Bakken, C. Adamo, J. Jaramillo, R. Gomperts, R. E. Stratmann, O. Yazyev, A. J. Austin, R. Cammi, C. Pomelli, J. W. Ochterski, R. L. Martin, K. Morokuma, V. G. Zakrzewski, G. A. Voth, P. Salvador, J. J. Dannenberg, S. Dapprich, A. D. Daniels, Ö. Farkas, J. B. Foresman, J. V. Ortiz, J. Cioslowski, D. J. Fox, Gaussian 09, Revision A.01; Gaussian, Inc.: Wallingford, CT, USA, 2009.

[18] (*a*) C. L. Covington, P. L. Polavarapu, *J. Phys. Chem*. A, **2013**, *117*, 3377; (*b*) D. K. Derewacz, C. R. Mcnees, G. Scalmani, C. L. Covington, G. Shanmugam, L. J. Marnett, P. L. Polavarapu, B. O. Bachmann, *J. Nat. Prod*. **2014**, *77*, 1759.

[19] (*a*) J. Shen, C. Zhu, S. Reiling, R. Vaz, *Spectrochim. Acta, Part A*, **2010**, *76*, 418; (*b*) C. L. Covington, P. L. Polavarapu, "CDSpecTech: Computer programs for calculating similarity measures of comparison between experimental and calculated dissymmetry factors and circular intensity differentials," https://sites.google.com/site/cdspectech1/: 2014.

[20] (*a*) P. L. Polavarapu, C. L. Covington, *Chirality*, **2014**, *26*, 539; (*b*) J. Vandenbussche, P. Bultinck, A. K. Przybyl, W. A. Herrebout, *J Chem. Theory. Comput*., **2013**, *9*, 5504

[21] (a) A. Hajra, N. Yoshikai, E. Nakamura, *Org. Lett.*, **2006**, *8*, 4153. (b) S. Halbert, H. Gérard, *New J. Chem.*, **2015**, *39*, 5410. (c) S. Drissi-Amraoui, T. E. Schmid, J. Lauberteaux, C. Crévisy, O. Baslé, R. Marcia de Figueiredo, S. Halbert, H. Gérard, M. Mauduit, J.-M. Campagne, *Adv. Synth. Cat.,* **2016**, *358*, 2519.

[22] a) E. Nakamura, S. Mori, K. Morokuma, *J. Am. Chem. Soc.* **1997**, *119***,** 4900; b) A. Hajra, N. Yoshikai, E. Nakamura, *Org. Lett.* **2006**, *8*, 4153; c) N. Yoshikai, E. Nakamura, *Chem. Rev.* **2012**, *112*, 2339.

[23] A. Alexakis, J. E. Bäckvall, N. Krause, O. Pamies, M. Diéguez, *Chem. Rev.,* **2008**, *108*, 2796.

[24] (*a*) M. d'Augustin, A. Alexakis, *Chem. Eur. J.*, **2007**, *13*, 9647; (*b*) M. Vuagnoux-d'Augustin, L. Palais, A. Alexakis, *Angew. Chem. Int. Ed.*, **2005**, *44*, 1376.

[25] P. L. Polavarapu, *Chirality*, **2008**, *20*, 664.

[26] D. Tran Ngoc, M. Albicker, L. Schneider, N. Cramer, *Org. Biomol. Chem.*, **2010**, *8***,** 1781.

[27] A. Homs, M. E. Muratore, A. M. Echavarren, *Org. Lett*., 2015, **17**, 461.

[28] (*a*) E. Piers, B. W. A. Yeung and F. F. Fleming, *Can. J. Chem*., **1993**, *71*, 280; (*b*) E. Piers, B. W. A. Yeung, *J. Org. Chem*. **1984**, *49*, 4567.

[29] For the geminal dimethylation of carbonyls, see: M. T. Reetz, J. Westermann, R. Steinbach, *Angew. Chem. Int. Ed*., **1980**, *19*, 900.

FULL PAPER

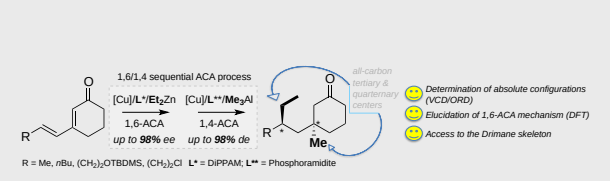

A stereo-controlled Cu-catalyzed sequential 1,6/1,4-ACA of C-metalated hard nucleophiles to cyclic dienones is reported. High ee's and de's were reached, thus affording enantio-enriched 1,3-dialkylated moieties. The absolute configurations were determined using VCD and ORD spectroscopy, in combination with DFT calculations and X-Ray analysis. Interestingly, DFT calculations of the mechanism for the enantioselective 1,6-addition via an unprecedented Cu-Zn bimetallic catalytic system confirmed this attribution. This methodology was applied to the synthesis of drimane skeleton.

C. Blons, M. S. T. Morin, T. E. Schmid, T. Vives, S. Colombel-Rouen, O. Baslé, T. Reynaldo, C. L. Covington, S. Halbert, S. N. Cuskelly, P. V. Bernhardt, C. M. Williams, J. Crassous,* P. L. Polavarapu,* C. Crévisy,* H. Gérard,* M. Mauduit**

Page No. – Page No.

Asymmetric Sequential Cu-Catalyzed 1,6/1,4 Conjugate Additions of Hard Nucleophiles to Cyclic Dienones. Determination of Absolute Configurations and Origins of Enantioselectivity